Journal of Nuclear Materials 475 (2016) 227–236

Contents lists available at ScienceDirect

Journal of Nuclear Materials

journal homepage: www.elsevier.com/locate/jnucmat

Effect of different lay-ups on the microstructure, mechanical properties and neutron transmission of neutron shielding fibre metal laminates

Xuelong Fu [a, b], Xiaobin Tang [a], Yubing Hu [a], Huaguan Li [a], Jie Tao [a, *]

[a] College of Material Science & Technology, Nanjing University of Aeronautics & Astronautics, Nanjing, 211100, China
[b] Department of Mechanical and Electronic Engineering, Jiangsu Polytechnic of Finance & Economics, Huai'an, 223003, China

HIGHLIGHTS

- A novel neutron shielding fibre metal laminates (NSFMLs) with different lay-ups was successfully fabricated using hot molding process.
- Mechanical properties of the NSFMLs were performed in accordance with relative standards.
- Neutron transmission of the NSFMLs was conducted according to the testing results.
- The effect of carbon fibres on the neutron transmission of the NSFMLs was also investigated.

ARTICLE INFO

Article history:
Received 5 January 2016
Received in revised form
15 March 2016
Accepted 13 April 2016
Available online 14 April 2016

Keywords:
Neutron shielding fibre metal laminates (NSFMLs)
Neutron shielding composite
Mechanical properties
Neutron transmission

ABSTRACT

A novel neutron shielding fibre metal laminates (NSFMLs) with different lay-ups, composed of stacking layers of AA6061 plates, neutron shielding composite and carbon fibre reinforced polyimide (CFRP), were fabricated using hot molding process in atmospheric environments. The microstructure, mechanical properties and neutron transmission of the NSFMLs were evaluated, respectively. The results indicated that the NSFMLs possessed good mechanical properties owing to the good interfacial adhesion of the components. Tensile strength and elastic modulus of the NSFMLs increased with the numbers of lay-ups, while the elongation to fracture exhibited obvious declining tendency. Flexural strength and modulus of the NSFMLs were improved obviously with the increasing of stacking layers. Neutron transmission of the NSFMLs decreased obviously with increasing the number of lay-ups, owing to the increase of ^{10}B areal density. Besides, the effect of carbon fibres on the neutron shielding performance of the NSFMLs was also taken into consideration.

1. Introduction

Owing to the rapid economic and demographic growth in the world, all countries around the world have taken measures to meet the rapidly growing energy needs of human beings [1,2]. Especially in the new round of national planning, China promotes the usage of nuclear energy and other renewable energy in order to alleviate the contamination of the surrounding environment and contribute to a more sustainable development [3,4]. Although the nuclear fuel could not yield carbon dioxide or other harmful greenhouse gas emissions, it creates its own waste in the form of highly radioactive spent nuclear fuel (SNF) enriched in the fissile ^{235}U. Therefore, it is very important to pay close attention to the management of SNF waste. At present, there are three kinds of disposal for spent nuclear fuel: (1) wet pool storage [5], (2) dry cask storage [6] and direct reusage [7]. Although wet pool storage as interim storage is the most convenient storage mode, it occupies a lot of space with high cost assessment, while metal cask storage marks the highest efficiency for the facilities [8]. Most of the inventory is destined for long-term storage and eventual geologic disposal, which is stored in the storage rack or cask. Normally, spent fuel storage rack or cask should have good mechanical properties, corrosion resistance, low-velocity impact resistance, low coefficient of thermal expansion, aging resistance and high temperature performance to a certain degree [9–11].

* Corresponding author. Department of Material Science & Technology, Nanjing University of Aeronautics and Astronautics, Nanjing, China.
E-mail address: taojie@nuaa.edu.cn (J. Tao).

http://dx.doi.org/10.1016/j.jnucmat.2016.04.021
0022-3115/

Usually, spent nuclear fuel emits fast neutrons which can be decelerated and transformed into thermal neutrons as they collide with matters, therefore, neutron shielding materials must have the performance of reducing the fast neutrons and absorbing the thermal neutrons. Nowadays, the neutron shielding materials are mainly focused on the preparation of boron-containing polyethylene [12], boron-containing stainless steel [13,14], Al/B, Fe/Al/B [15,16], glass fibre/boron carbide (B_4C) epoxy resin composite [17] and a novel LiF, Sm_2O_3, Gd_2O_3/carbon fibre/polyimide material [18]. Among these neutron shielding materials, boron carbide (B_4C) as one of the promising elements has been widely studied, mainly because it is relatively cheap and contains the high thermal neutron absorbing cross-section element ^{10}B with natural abundance of 19.9% [15]. Normally, the fraction of boron carbide contained in the composite is no more than 30 wt%, otherwise the mechanical performance of the composite is seriously degraded. On the other hand, polymers as a neutron moderator are always used to slow down the fast neutrons as a function of its high volume fraction of hydrogen atoms, such as polyethylene (PE), epoxy (EP) and polyimide (PI) [19]. The problem is that the melting point of PE or EP is so low that it can hardly withstand the high temperature generated from the SNF, while the operating condition of polyimide resin ranges from −200 to 300 °C and initially decomposes at 500 °C. Ployimide (PI) resin with good radiation resistance can endure high temperature for several hours even though the heat exchange system of nuclear facilities loses its function, because it has good thermal resistance at elevated temperatures. However, it possesses lower mechanical properties with 60 MPa of tensile strength, 3.8 GPa of flexural modulus and 27 J/m of impact strength. Therefore, it is necessary to prepare a new kind of neutron shielding material with different structure which can make full use of polyimide's advantages and minimize its disadvantages.

In this study, neutron shielding fibre metal laminates (NSFMLs) with different lay-ups were successfully fabricated using hot molding process. The microstructure and mechanical properties of NSFMLs were performed in detail, and the effect of different lay-ups on the tensile and flexural properties and neutron transmission ratio of NSFMLs were also investigated in order to find out the relationship between structure and mechanical properties and probe the tendency of neutron shielding performance with the increasing of the lay-ups.

2. Experimental procedure

2.1. Materials

AA6061-T6 aluminum alloy plates (thickness 0.5 mm, Southwest Aluminum (Group) Co. Ltd., China), nuclear-grade boron carbide (B_4C) particles (average particle size 7.5 μm, 99.5% in purity, Jingangzuan Boron Carbide Co. Ltd., Mudanjiang, China), carbon fibre (TR50S 6K, Mitsubishi Rayon Co. Ltd., China) and PMR polyimide resin (KH-308, Institute of Chemistry, Chinese Academy of Science) were used as starting materials. The chemical composition of AA6061 aluminum alloy plate is shown in Table 1 and the micrograph of B_4C particulates is presented in Fig. 1. The PMR polyimide contains 50 wt.% of polymerized reaction mixtures. Carbon fibre reinforced prepregs (CFRP) with the thickness of 0.125 mm, which were composed of carbon fibre and PMR polyimide, were self-prepared by numerical control automatic placement machine in the laboratory [11].

Table 1
Chemical composition of AA6061 aluminum alloy.

Element	Si	Fe	Cu	Mn	Mg	Cr	Zn	Ti	Al
wt%	0.64	0.48	0.33	0.15	1.10	0.3	0.25	0.15	Bal.

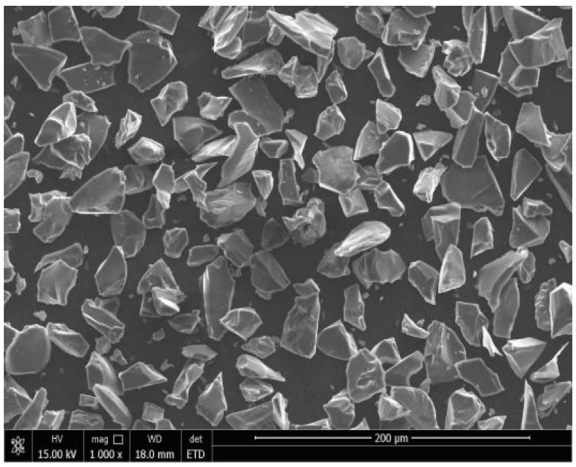

Fig. 1. SEM micrograph of boron carbide particles with average particle size of 7.5 μm.

2.2. Preparing process

AA6061 aluminum alloy plates were firstly anodized by phosphoric acid according to the standard procedures [20], and then coated with neutron shielding composite with 0.2 mm in thickness, which was composed of the mixture of PMR polyimide resin and nuclear-grade boron carbide particles. The fraction of B_4C particles contained in the neutron shielding composite was about 50 wt.%. AA6061 plates coated with neutron shielding composite were then put into the drying oven so as to get rid of the solvent. After completing the whole process mentioned above, the specimens were covered with carbon fibre reinforced prepregs (CFRP). Each prepreg layer was composed by two unidirectional carbon fibre prepreg piled-up at 0°, which was coincident with the rolling direction of AA6061 sheets.

Neutron shielding fibre metal laminates (NSFMLs) with the configuration of 2/1, 3/2, 4/3 and 5/4 were prepared with stacking layers of AA6061 alloy plates, neutron shielding composite and carbon fibre reinforced prepregs (CFRP), and a schematic representation of their lay-ups in detail is illustrated in Fig. 2. The typical cross section of NSFML with the configuration of 3/2 is presented in Fig. 2(e).

The neutron shielding metal laminates (NSFMLs) were preprocessed by hand lay-up and put into the compression mold, and then placed into the vulcanizing machine. The explicit curing process of fibre metal laminate is illustrated in Fig. 3. After completing the whole curing process, the electricity was shut down, while packing pressure should be maintained in order to alleviate the impact of residual strength on the mechanical properties of the NSFMLs. The specimens with different dimensions were cut using high precision Struers Cutter Secotom-15 (cutting tool: diamond saw blade, 200 × 0.8 × 22 mm; feed rate: 0.15–0.25 mm/s; rotation speed: 3200 rpm). Owing to the high hardness and non electrical conductivity of boron carbide particulates, it is undesirable to handle the specimens with Numerical Control (NC) machining and Wire Electrical Discharge Machining (WEDM).

2.3. Material analysis and characterization

The mechanical testing include tensile, flexural and floating roller peel strength were conducted on the CMT-5015 Universal

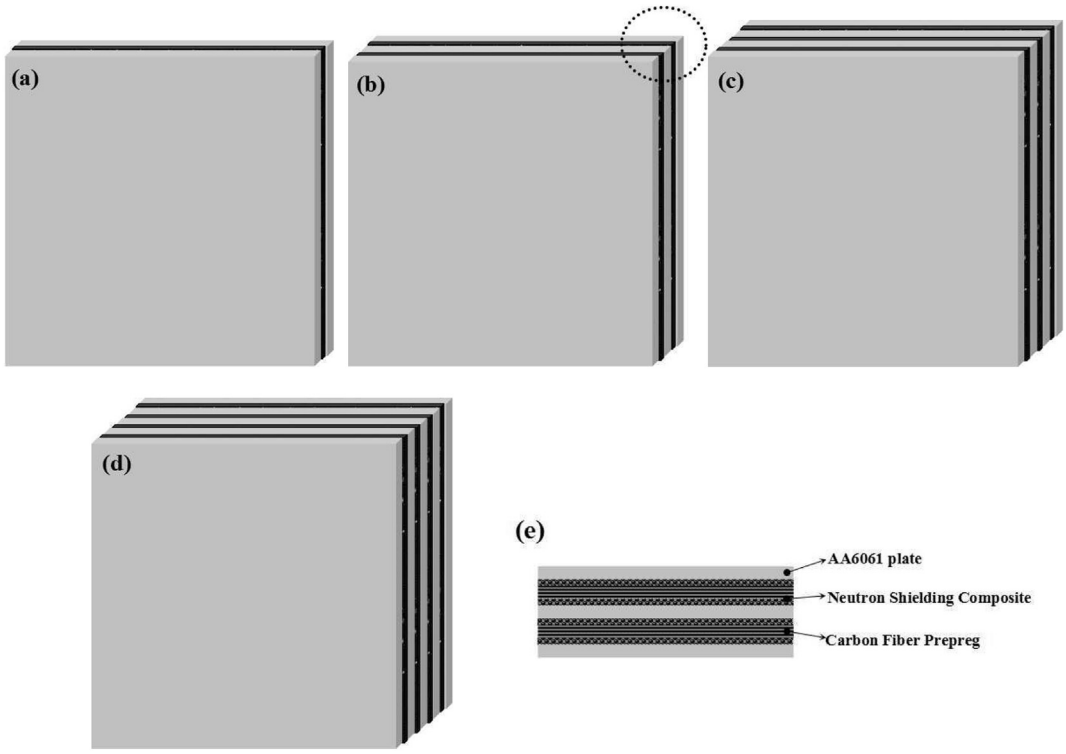

Fig. 2. Schematic representation of neutron shielding fibre metal laminates with different lay-ups: (a) 2/1; (b) 3/2; (c) 4/3; (d) 5/4; (e) cross section of the NSFML with the configuration of 3/2.

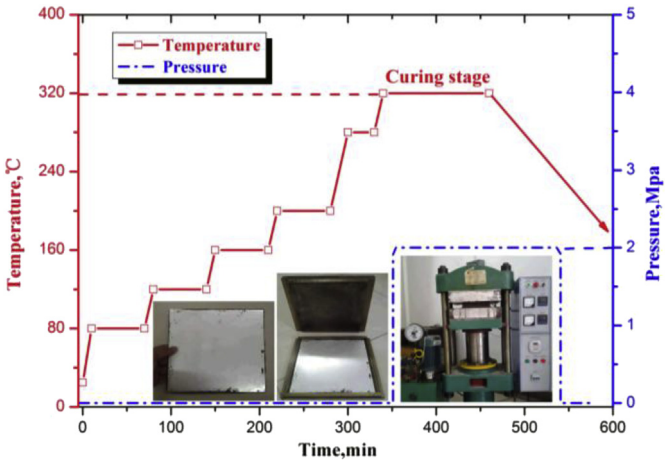

Fig. 3. Curing process of neutron shielding fibre metal laminates with the evolution of time.

Testing Machine (UTM) in displacement control, in accordance with ASTM D3039, ASTM D790 and ISO 4578 standards, respectively. The failure behavior and mechanism were also analyzed, which is very crucial to the stability and durability of the NSFMLs. Tensile properties of the specimens with the dimensions of 175 mm × 25 mm × (1.64–5.07) mm were monitored by extensometer in order to precisely measure the change of stress-strain curve at a displacement rate of 2 mm/min. The flexural properties were evaluated using a three-point bending test with a span to thickness ratio (L/h) of 32 at a crosshead displacement rate of 1 mm/min. The floating roller peeling test provided the average peeling load between the metal layers and neutron shielding composite, applying with a crosshead rate of 100 mm/min. All specimens were conditioned at room temperature (RT) with a relative humidity of 55%. Microstructures of the NSFMLs with different lay-ups were examined using optical microscope (OM, Leica DM IL LED, Germany) and field emission scanning electron microscopy (FE-SEM, Quanta 250 FEG, FEI, America) equipped with energy-dispersive spectroscopy (EDS, Oxford INCA energy).

2.4. Neutron transmission performance

The neutron shielding characteristics were evaluated based on thermal neutron transmission test, which was conducted on the ^{241}Am–Be neutron source with the intensity of 1.11 × 10^{10} Bq. Fig. 4 exhibits the schematic diagram of neutron transmission experiment. Neutron ray first penetrated through a 30 mm-thick lead plate and passed through a polyethylene plate (30 mm thick), and

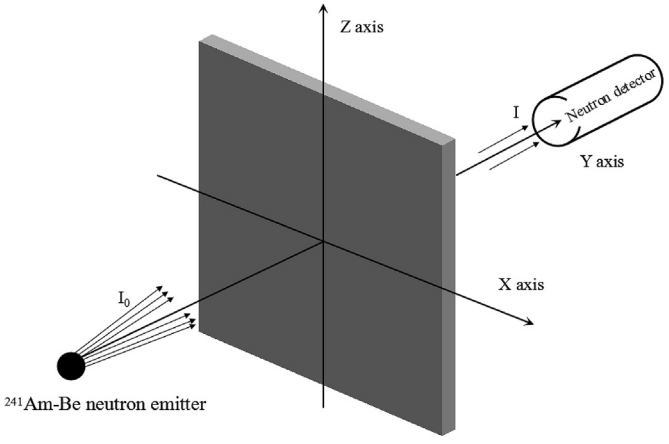

Fig. 4. Schematic representation of neutral transmission of the NSFMLs.

then passed through the NSFML specimens, finally, was detected using an He-3 proportional counter with 12.5 mm in diameter. The distance between the neutron emitting source and detector was 300 mm. The duration of each measurement lasted for 10 s and each specimen was tested for 5 times, and then the results were averaged. The neutron permeability (η) of the NSFMLs was calculated using the following equation [21]:

$$\eta = \frac{I - I_e}{I_0 - I_e} = e^{-\sum_t \cdot x}$$

where I is the neutron transmission intensity, I_0 is the incident intensity of the neutron, I_e is the environmental intensity of the neutron. Σ_t is the total macroscopic cross sections and x is the thickness of the specimen.

3. Results and discussion

3.1. Microstructure characteristics

Optical micrographs of neutron shielding fibre metal laminates (NSFMLs) with the configuration of 2/1, 3/2, 4/3 and 5/4 are shown in Fig. 5. It can be clearly seen in the Fig. 5(a)-(d) that the structures of the NSFMLs with different lay-ups are very flat and the thickness of interlayer is uniform under low magnification, and the good interface between AA6061 plates and neutron shielding composite can also be observed. Because the surface of AA6061 plates were proceeded with the anodic oxidation process, porous structure was formed on the surface of AA6061 alloy plates so that neutron shielding composite flowed into the hollow and crystallized in the process of hot pressing. As shown in the Fig. 5(e) and (f), boron carbide particulates and carbon fibres are tightly enclosed by the PMR polyimide resin, because the applied load is high enough to promote the natural flow of PMR resin and remove the gas entrapped in the NSFMLs. Moreover, the suitable curing process is very important for the preparation of the NSFMLs, which can drastically improve the wettability between B_4C particles and polyimide (PI) resin and reduce the internal porosity of the composite laminates. The uniform distribution of boron carbide particles in the neutron shielding composite is presented in Fig. 5(g), and it is a prerequisite for high performance of neutron shielding materials.

3.2. Mechanical properties

3.2.1. Tensile strength

Fig. 6 shows that the tensile strength and elastic modulus of the NSFMLs increase with the numbers of the lay-ups, while the elongation to fracture exhibits obvious declining tendency. The reason for this phenomenon can be essentially explained by theoretical calculation using the relationship proposed by M.S.Pma [22]:

$$MVF = \frac{\sum_t^p t_{Al}}{t_{lam}} \quad (1)$$

$$FVP = \frac{\sum_t^p t_{FRP}}{t_{lam}} \quad (2)$$

$$E_{lam} = MVF \cdot E_{Al} + FVP \cdot E_{FRP} \quad (3)$$

$$\sigma_{lam} = MVF \cdot \sigma_{Al} + FVP \cdot \sigma_{FRP} \quad (4)$$

where MVF is the metal volume fraction, FVP is the volume fraction of carbon fibre reinforced composite and p is the number of ply. The t_{Al}, t_{lam}, t_{FRP} refer to the thickness of single AA6061 alloy plate, fibre metal laminates and fibre reinforced polymers, respectively. The necessary mechanical property parameters of all the constituents for calculations are given in Table 2.

From the formula (4) mentioned above, it can be clearly seen that tensile properties of the NSFMLs mainly depend on the volume fraction of the components in the NSFMLs. While the tensile strength of carbon fibre is much higher than that of AA6061 sheets, consequently, tensile performance of the NSFML is mainly determined by the volume fraction of carbon fibre. On the other hand, the elongation of carbon fibre is much lower than that of AA6061 alloy plate and the carbon fibre reinforced prepreg(CFRP) is very fragile, indicating that the NSFML's elongation tends to decline with the increasing of carbon fibre fraction. In other words, enhancement in strength and decrease in elongation are by virtue of the increment of volume fraction of carbon fibre in the NSFML materials. The authors in the literature [23] investigated the influence of interfacial bonding on the tensile ductility of multi-layered steels, indicating that the tensile elongation of laminated composites was improved with the strong interface. When comparing the testing results with other studies using different preparation scheme, tensile properties of the NSFMLs are much higher than that of AA6061/B_4C composite prepared by vacuum hot pressing followed by hot rolling [9] and HDPE/B_4C composite prepared by hot extrusion [24]. For the NSFMLs, the main concern is to eliminate the residual stress and avoid the delamination in order to ensure the durability and reliability of neutron shielding laminated composites.

In addition to mechanical characterization, a morphological analysis of fractured samples was performed in order to determine the fracture mechanism. Fig. 7 shows the tensile fractographs of the NSFMLs in different areas. Fig. 7(a), (b) exhibit the fracture images of carbon fibre reinforced prepregs, indicating the good bonding between carbon fibres and PMR polyimide resin after hot molding process (Fig. 7(b)). When the specimens reached to the yield point and fractured as a function of tensile stress, carbon fibres were substantially pulled out from the PMR polyimide resin causing a plenty of voids emerged in the NSFMLs, as shown in Fig. 7(a) and (c). The interface debond between AA6061 alloy sheet and neutron shielding composite was observed during the tensile process, as a function of their differences in ductility. Meanwhile, the fractograph of the neutron shielding composite containing B_4C particles presented a good interfacial bonding between B_4C particles and PMR polyimide, as illustrated in Fig. 7(d). Fig. 7(e) exhibits the fractograph of AA6061 plate in the NSFMLs with the configuration of 4/3, and the tensile fracture is dimple cleavage owing to the good ductility of AA6061 alloy plate.

3.2.2. Flexural strength

Fig. 8 presents the testing results of the flexural properties of NSFML with different lay-ups. The results indicated that, with regard to the NSFMLs with the configuration ranging from 2/1 to 5/4, the flexural strengths were 389 MPa, 424 MPa, 431 MPa and 448 MPa, respectively. The flexural strength of the NSFMLs with different lay-ups increased with the increasing of alternate layers. As for the flexural modulus, it indicated a remarkable increase in flexural modulus values obtained from the testing results. The flexural modulus of NSFML with the configuration 5/4 was 50 GPa, which was about 2 times than that with the configuration of 2/1. As a result, the NSFMLs with more complicated configuration have a

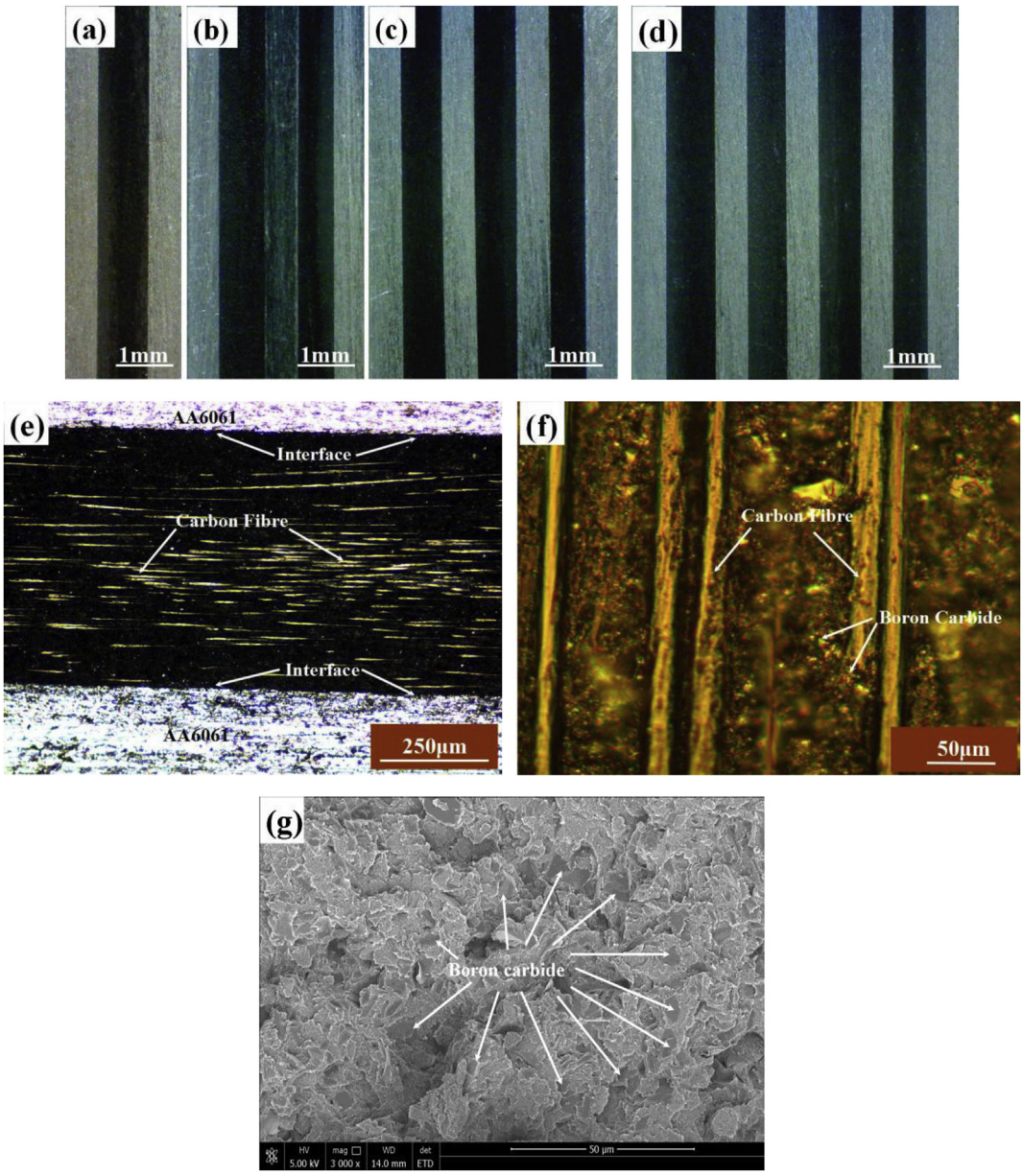

Fig. 5. Optical and SEM micrographs of neutron shielding fibre metal laminates with different configuration: (a) 2/1; (b)3/2; (c)4/3; (d)5/4; (e) micrograph of AA6061 and the CFRP under high magnification; (f) micrograph of boron carbide and carbon fibre; (g)SEM micrograph of the distribution of boron carbide particles in the neutron shielding composite.

better capacity of resisting the bending deformation.

Fig. 9 shows the micrographs of NSFML samples with different lay-ups after flexural testing. Owing to the maximum deflection of central point as a function of applied load, most samples presented in the Fig. 9(a)-(d) broke up at the middle of the NSFMLs, which was also the typical characteristic of bending failure. Almost all samples exhibited the same tendency of failure mode. When the applied load exceeded over ultimate bending strength of the NSFMLs, the outermost layer firstly broke as a function of the mechanics characteristic of the specimens. Owing to carbon fibre reinforced composite with high brittleness, the breakage originated from the outermost carbon fibre/PMR composite layer, while the outer AA6061 plate layer did not fracture by virtue of its high ductility. For the NSFML with the configuration of 2/1, there was no delamination for the specimen presented in Fig. 9(a), because the inner AA6061 plate can effectively transfer the applied load to the outer plate through neutron sheilding composite layer and the inner

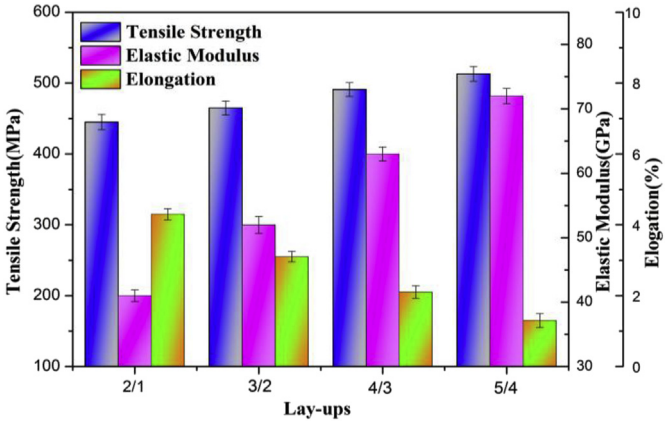

Fig. 6. Tensile properties of neutron shielding fibre metal laminates with different lay-ups.

Table 2
Material properties of the constituents.

Materials		σ_{lam} (MPa)	E_{lam} (GPa)	$\sigma_{lam,t}$ (MPa)	$E_{lam,t}$ (GPa)	FVP (%)
NSFMLs	2/1	445	41	488	59	15.2
	3/2	467	52	516	67	17.9
	4/3	491	63	528	78	19
	5/4	513	72	541	86	19.7

$\sigma_{lam,t}$ and $E_{lam,t}$ are the theoretical results of mechanical properties of composite laminates.

plates generate enough plastic deformation to make them as a whole. With the increasing of the plies, the applied stress induced the delamination between the neutron shielding composite layer and AA6061 plates, as shown in Fig. 9(b), (c), and (d). After comparing the fracture characteristics of NSFML with different lay-ups, the delamination was inclined to present more seriously for the NSFML with the configuration 4/3 and 5/4, as presented in Fig. 9(c) and (d). It can be conferred that, when the applied force exerts on the specimens, the outer layers away from the mesosphere are inclined to subject to higher flexural strength, causing the delamination of the NSFMLs obviously.

3.2.3. Peel strength

Normally, peel strength of the NSFML is mainly determined by the interaction of several factors: the molding process, interfacial bonding between adhesives and relative boundary and the

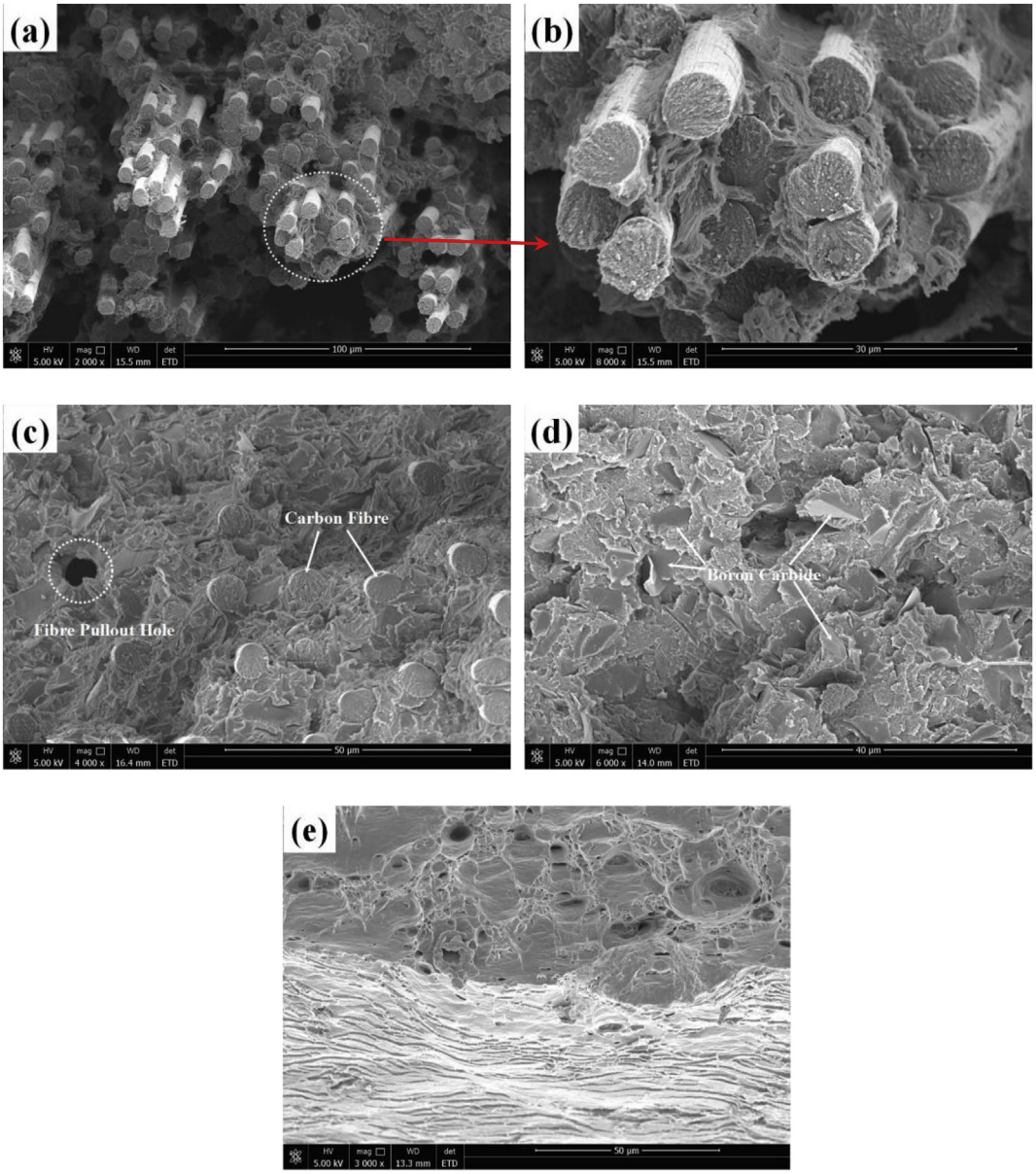

Fig. 7. Tensile fracture morphology of the NSFMLs with different areas: carbon fibre reinforced prepregs with (a) low magnification and (b) high magnification; (c) pullout hole in the laminates; (d) fractograph of neutron shielding composite; (e) fractograph of AA6061 plate.

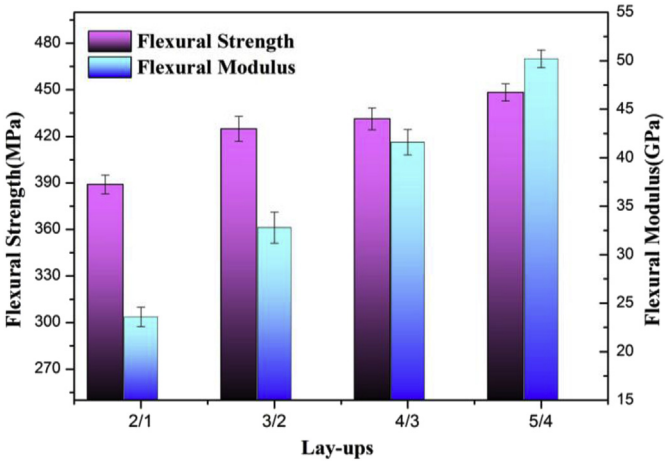

Fig. 8. Flexural properties of hybrid fibre metal laminates with different lay-ups.

flexibility of adhesives itself [25]. Fig. 10 shows the peel strength distribution of the NSFMLs with 50 wt% of boron carbide obtained from the experiment. For comparison, the NSFML coated with neat PMR polyimide which was used to substitute for the neutron shielding composite was also prepared. It can be clearly seen from Fig. 10(a) that the peel strength of NSFML with neat PMR polyimide is about 4.89 N mm^{-1}, while for the NSFML containing 50 wt.% of boron carbide particles that is about 2.52 N mm^{-1}. The discrepancy in peel strength was not so obvious for the NSFMLs with the configuration of 2/1, 3/2, 4/3, and 5/4. It can be seen from force-displacement curve of NSFML with the configuration of 4/3 in Fig. 10(b) that the peeling force of entire process appears to be lower on both sides but higher and more uniformly distributed in the middle.

Fig. 11 presents the SEM micrograph of stripping surface of the NSFMLs after peel testing. There was the presence of carbon fibre, boron carbide particles and resin debris on the peeled AA6061 alloy plate, as presented in Fig. 11(a) and (b). Normally, the interfaces between AA6061 plates and the neutron shielding composite layer are always weaker than that of carbon fibre and PMR polyimide, but

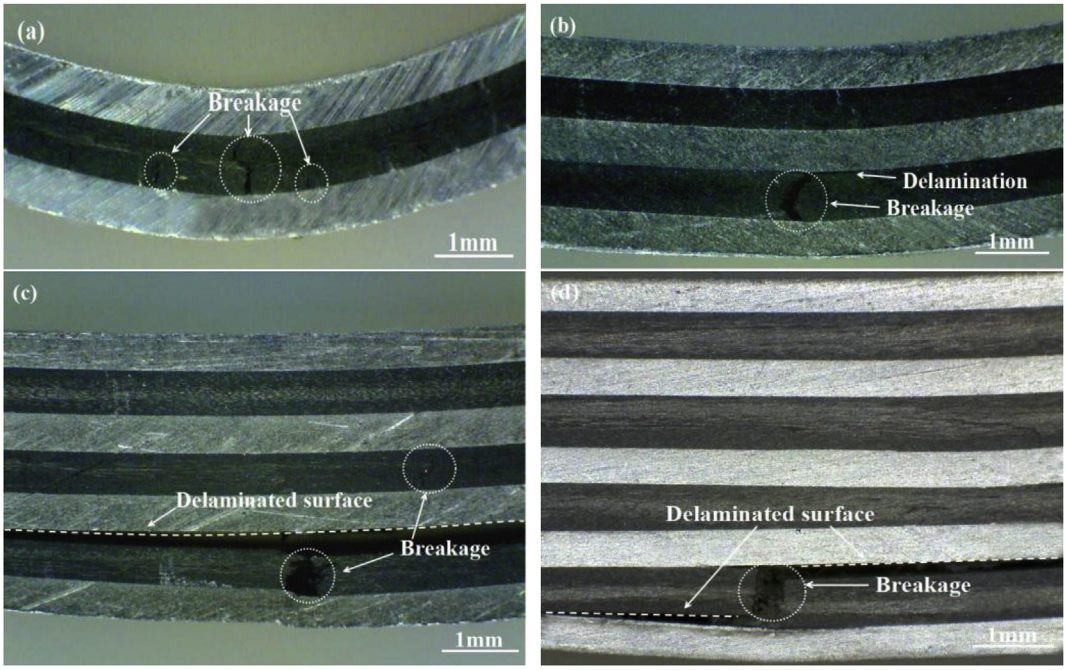

Fig. 9. Images of the NSFMLs with different lay-ups after flexural testing: (a)2/1; (b)3/2; (c)4/3; (d)5/4.

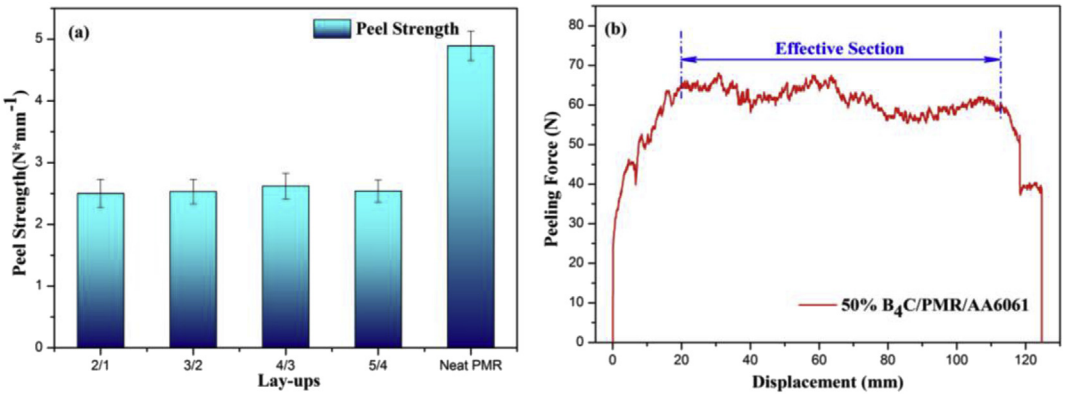

Fig. 10. (a) peel strength of the NSFMLs with different lay-ups; (b) force-displacement curve of NSFML with the configuration of 4/3.

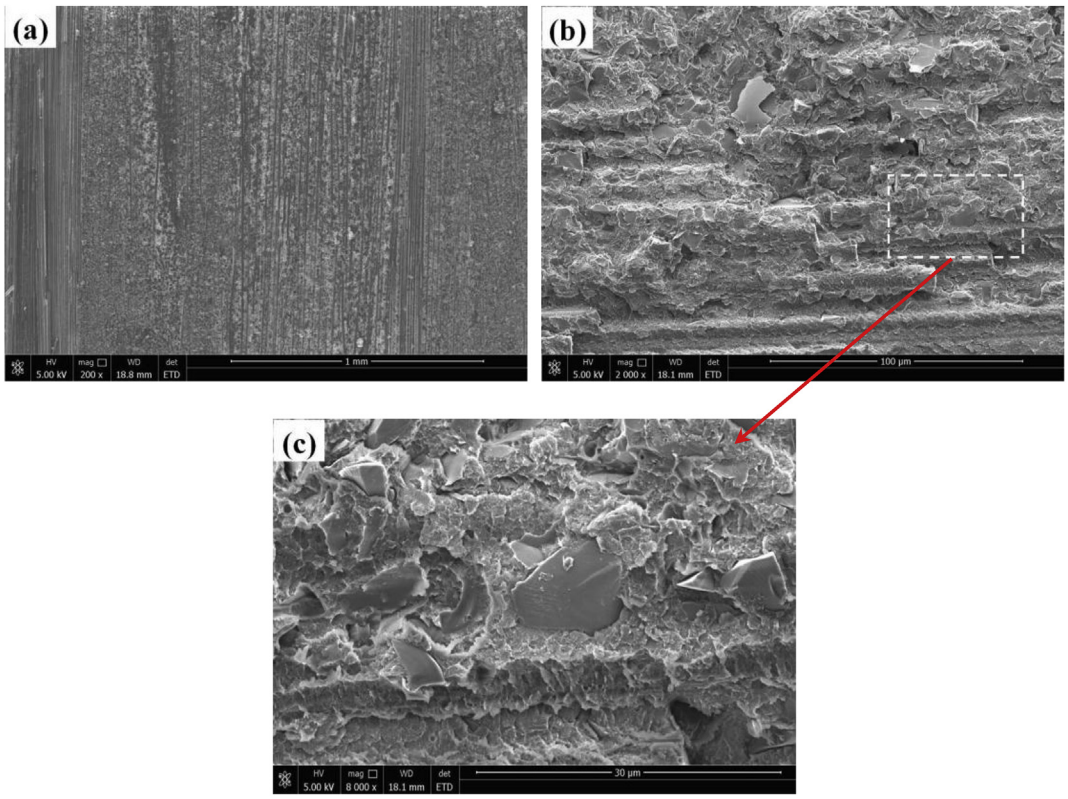

Fig. 11. SEM micrographs of (a) stripping surface of the NSFMLs after peel test; (b) under low magnification and (c) high magnification.

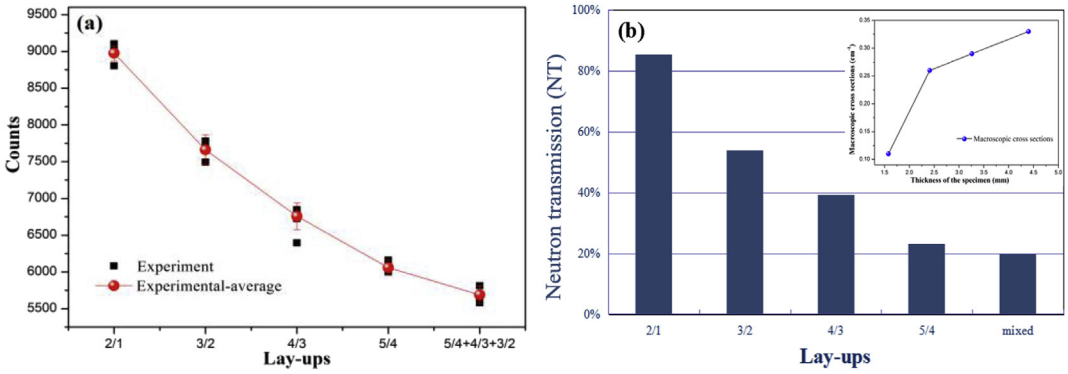

Fig. 12. Testing results as a function of different lay-ups: (a) testing value; (b) neutron transmission.

some carbon fibres are even broken up and peeled off from the composite layer in the study. As a result, the NSFMLs with different configuration display the desirable interfacial bonding properties between AA6061 plates and the neutron shielding composite layer [26].

3.3. Neutron transmission performance

Fig. 12 presents the testing results and neutron transmission as a function of different lay-ups, and the testing results were changed with the numbers of lay-ups. With increasing the thickness of the NSFMLs, neutron transmission for the specimens decreased sharply. The NSFMLs with the configuration of 5/4 had the neutron transmission ratio of 23.1%, which was obviously less than composite laminate with the configuration of 2/1. This can be explained by the fact that, when the thickness of the specimen is thin, thermal neutrons can be absorbed by the NSFMLs, but fast neutrons continue to transmit. The reason is that fast neutron absorbing cross section of boron carbide is very small, resulting in that fast neutrons can go through the materials without being shielded [27]. If further increasing the thickness of the specimens, hydrogen atoms in the polyimide resin have a direct impact on the fast neutrons and slow them down through elastic and inelastic scattering, as a result, fast neutrons transform into thermal neutrons which can be absorbed by ^{10}B element contained in the boron carbide particles. Moreover, the augment of ^{10}B areal density increases with the numbers of the NSFML's plies. It can be inferred that mass fraction of boron element and the ratio between hydrogen and boron carbide have a very important role in the neutron shielding efficiency of composite laminates. For the fast neutrons with the energy over 1 keV, mass fraction of hydrogen is the main influential factor that can largely affect the macroscopic cross section through elastic scattering. While for thermal neutrons with the energy below 0.025 eV, mass fraction of boron carbide

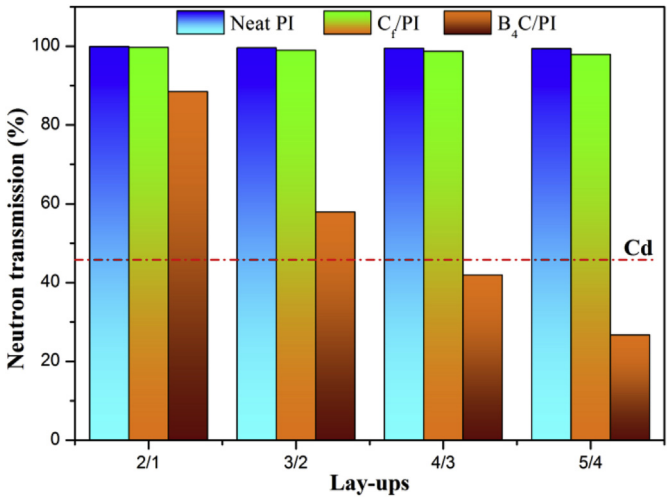

Fig. 13. Comparison result of neutron transmission of the FMLs with neat PI resin, C_f/PI without boron carbide and B_4C/PI resin without carbon fibre.

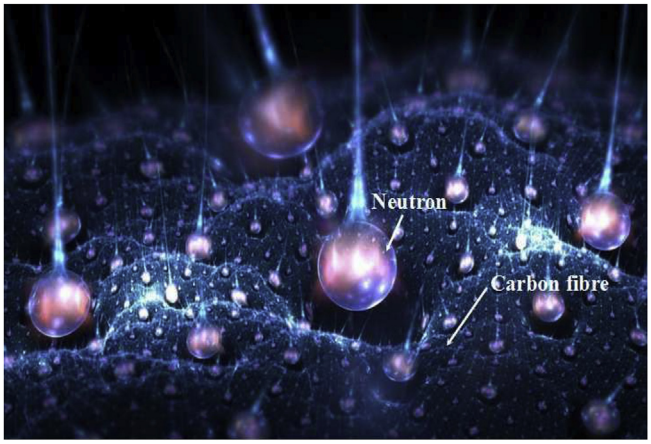

Fig. 14. Schematic of the interactions between neutrons and carbon fibre contained in the NSFML.

plays a decisive role [28]. Therefore, neutron transmission of the NSFMLs tends to decrease with the increasing of stacking layers. When compared with the counterparts, the NSFMLs exhibit better mechanical properties and capability of neutron absorption under the same conditions.

On the other hand, the effect of carbon fibre on the neutron shielding performance of fibre metal laminates (FMLs) was also explored. Neutron transmission of the composite laminates with and without carbon fibre inside (entitled as C_f/PI and neat PI, respectively) was tested and taken for comparison, and all specimens here contained no boron carbide particles in the neutron shielding composite layer. Besides, neutron transmission of the FML with 50% of boron carbide in the composite layer and without carbon fibre inside (entitled as B_4C/PI) was also investigated. The testing results are shown in Fig. 13. The NSFMLs with carbon fibre and boron carbon particles inside have a better neutron transmission ratio than the FMLs containing with 50 wt% of boron carbide and without carbon fibre, and the discrepancy between two different testing results is about 8%, which implies that carbon fibres play an important role in the process of neutron transfer. The neutron transmission for neat PI and C_f/PI specimen is over 99%, which highlights the importance of boron carbide as a neutron absorbent.

The reason lies in that, graphite as one of the carbon isotopes, contained in carbon fibres, has a high neutron reflective cross section. And it is also a good neutron moderator, which can increase the number of effective collisions between neutrons and atoms and promote the absorption of thermal neutrons [29]. When the thickness of the NSFML is thin, the fast neutrons can easily penetrate through the plates without being shielded or moderated, and a small quantity of thermal neutrons can be absorbed by the 10B elements contained in the NSFMLs. The probability of collision between incident neutrons and graphite in the carbon fibre is improved with increasing the thickness of the NSFMLs, and the fast neutrons with high energy can be slowed down through elastic collision with carbon fibre, resulting in the absorption of thermal neutron by ^{10}B elements. The schematic interaction between neutrons and carbon fibre is illustrated in Fig. 14. Generally speaking, carbon fibres contained in the NSFML have a positive role in the process of neutron shielding.

4. Conclusion

In this investigation, the NSFMLs with different lay-ups were fabricated using hot molding process. Boron carbide particles were uniformly distributed in the NSFMLs and the good interface of the NSFMLs was also observed. The tensile strength and elastic modulus of NSFMLs increased with the numbers of the lay-ups, while the elongation to fracture exhibited obvious declining tendency, owing to the increment of carbon fibre in the NSFML materials. Flexural strength and modulus of the NSFMLs with different lay-ups increased with the increasing of stacking layers, and the delamination for the specimens with multi-layers presented more seriously. When the applied stress, exceeding over the ultimate bending strength, was exerted on the specimen, the outermost layers away from the mesosphere were inclined to subject to higher flexural strength, leading to the obvious delamination of the NSFMLs.

The neutron transmission ratio decreased sharply with the increasing of the lay-ups, owing to the increase of ^{10}B areal density in the NSFMLs. The neutron transmission ratio varied from 85.2% to 23.1%, when the configuration of the NSFMLs changed from 2/1 to 5/4. Besides, carbon fibres as a neutron moderator have a direct effect on the neutron shielding performance of the NSFMLs, and neutron transmission of composite laminates without carbon fibre was increased by 8% when compared with that of the NSFMLs containing with boron carbide and carbon fibre inside.

Acknowledgements

The authors gratefully acknowledge the financial support from the Fund of Jiangsu Innovation Program for Graduate Education, the Fundamental Research Funds for the Central Universities (No.KYLX_0258), Opening Project of Jiangsu Key Laboratory of Advanced Structural Materials and Application Technology (ASMA201401), and a Project Funded by the Priority Academic Program Development of Jiangsu Higher Education Institutions. Finally, thank prof. Jia Wenbao, from NUAA, for the help in the neutron shielding tests.

References

[1] R.G. Abrefah, S.A. Birikorang, B.J.B. Nyarko, Prog. Nucl. Energy 77 (2014) 84–91.
[2] Sara Al Saadi, Yongsun Yi, Ann. Nucl. Energy 75 (2015) 527–535.
[3] J.L. Wang, Z. Wan, Prog. Nucl. Energy 78 (2015) 47–55.
[4] F. Fiori, Z. Zhou, Ann. Nucl. Energy 83 (2015) 246–257.
[5] Chun-Hyung Cho, Tae-Man Kim, Ki-Yeoul Seong, Ann. Nucl. Energy 38 (2011) 976–981.

[6] Rodney C. Ewing, Nat. Mater. 14 (2015) 252–257.
[7] Nader M.A. Mohamed, Nucl. Eng. Des. 278 (2014) 182–189.
[8] W. Gudowski, Nucl. Phys. A 752 (2005) 623–632.
[9] H.S. Chen, W.X. Wang, Y.L. Li, et al., J. Alloy Compd. 632 (2015) 23–29.
[10] G. Odegard, M. Kumosa, Compos. Sci. Technol. 60 (2000) 2979–2988.
[11] Y.B. Hu, H.G. Li, L. Cai, et al., Compos. Part B Eng 69 (2015) 587–591.
[12] J.X. Lu, J.T. Chen, Nucl. Power Eng. 15 (1994) 370–374.
[13] J.C. Kuang, Z.Q. Jiang, S.Y. Zhang, et al., China Foundry 6 (2008) 32–36.
[14] M. Bastürk, J. Arztmann, W. Jerlich, et al., J. Nucl. Mater. 341 (2005) 189–200.
[15] J. Abenojar, M.A. Martinea, F. Velasco, J. Alloy Compd. 422 (2006) 67–72.
[16] J. Abenojar, A. Bautista, S. Guzmán, et al., Mater. Corros. 65 (2014) 678–684.
[17] F.D. Chen, X.B. Tang, P. Wang, et al., At. Energy Sci. Technol. 46 (2012) 703–707.
[18] P. Wang, X.B. Tang, F.D. Chen, et al., Nucl. Eng. Des. 284 (2015) 91–96.
[19] J.O. Iroh, K.M.S. Jordan, Surf. Eng. 16 (2000) 303–308.
[20] ASTM D3933-98, ASTM International, 2010.
[21] P. Zhang, Y.L. Li, W.X. Wang, et al., J. Nucl. Mater. 437 (2013) 350–358.
[22] A.S. Yaghoubi, B. Liaw, Compos. Struct. 94 (2012) 2585–2598.
[23] S. Nambu, M. Michiuchi, J. Inoue, et al., Compos. Sci. Technol. 69 (2009) 1936–1941.
[24] Ji Wook Shina, Jang-Woo Lee, Seunggun Yu, et al., Thermochim. Acta 585 (2014) 5–9.
[25] E. Njuhovic, A. Witt, M. Kempf, et al., Surf. Coat. Tech. 232 (2013) 319–325.
[26] H.G. Li, Y.B. Hu, Y.W. Xu, W.T. Wang, X.W. Zheng, H.B. Liu, J. Tao, Compos. Part B Eng 82 (2015) 72–77.
[27] Mark J. Rivard, Robert G. Zamenhof, Appl. Radiat. Isot. 61 (2004) 753–757.
[28] Z.F. Li, X.X. Xue, J. Northeast, Univ. Nat. Sci. 12 (2011) 1716–1720 (in chinese).
[29] X.Y. Chuan, X.L. Zhang, Carbon Tech. 28 (2009) 28–35 (in chinese).